Revealing Topological Superconductivity in Extended Quantum Spin Hall Josephson Junctions

Shu-Ping Lee,[1] Karen Michaeli,[2] Jason Alicea,[1] and Amir Yacoby[3]
[1]Department of Physics and Institute for Quantum Information and Matter, California Institute of Technology, Pasadena, California 91125, USA
[2]Department of Condensed Matter Physics, Weizmann Institute of Science, Rehovot 76100, Israel
[3]Department of Physics, Harvard University, Cambridge, Massachusetts 02138, USA
(Received 21 March 2014; published 6 November 2014)

Quantum spin Hall–superconductor hybrids are promising sources of topological superconductivity and Majorana modes, particularly given recent progress on HgTe and InAs/GaSb. We propose a new method of revealing topological superconductivity in extended quantum spin Hall Josephson junctions supporting "fractional Josephson currents." Specifically, we show that as one threads magnetic flux between the superconductors, the critical current traces an interference pattern featuring sharp fingerprints of topological superconductivity—even when noise spoils parity conservation.

DOI: 10.1103/PhysRevLett.113.197001 PACS numbers: 74.45.+c, 74.50.+r

Introduction.—"Spinless" one-dimensional (1D) topological superconductors [1–5] host various novel phenomena, most notably Majorana zero modes that lead to non-Abelian statistics and, in turn, fault-tolerant quantum information applications [6]. Among numerous plausible realizations [7–12], Fu and Kane's early proposal for nucleating 1D topological superconductivity at a quantum spin Hall (QSH)–superconductor interface remains a leading contender [13]. Experiments have, moreover, shown exciting recent progress with QSH behavior and good proximity effects conclusively demonstrated in both HgTe [14–18] and InAs/GaSb [19–22] quantum wells.

In light of these developments, the following question becomes paramount: How can one compellingly reveal topological superconductivity in these QSH setups? Most detection protocols to date focus on tunneling [23–25] and Josephson [7,26–36] anomalies. The latter originate from the fractional Josephson effect [1] wherein a phase twist $\delta\phi$ across a topological superconductor yields a supercurrent with 4π periodicity in $\delta\phi$—twice that of conventional junctions. One can view the doubled periodicity as arising from a pair of hybridized Majorana modes at the junction, which form an unusual Andreev bound state that mediates supercurrent via single electron (rather than Cooper pair) tunneling. In the simplest case this anomalous current takes the form $I_{4\pi} \propto (-1)^p \sin(\delta\phi/2)$, where the parity $p = 0, 1$ denotes the Andreev bound state's occupation number. Directly observing this spectacular effect is, however, nontrivial. Parity switching processes—which send $p \to 1 - p$ and can arise, e.g., from quasiparticle poisoning—restore 2π periodicity to the current unless measurements occur on a time scale short compared to the typical parity-flip time. (Long-time-scale measurements may still reveal subtler signatures of topological superconductivity [27,31,32,36], for instance through noise.)

Inspired by recent experiments by Hart *et al.* [18], we study transport in an extended Josephson junction bridged by a QSH insulator; see Fig. 1. This setup is expected to host two 1D topological superconductors that produce "parallel" fractional Josephson currents at the junction ends. One virtue of such extended junctions is that the critical current $I_c(\Phi)$, measured as a function of magnetic flux Φ passing between the superconductors, displays an interference pattern that can reveal detailed information about the nature of current flow. Here we ask whether such interference measurements can provide fingerprints of 1D topological superconductivity.

Our central result is that the fractional Josephson effect indeed imprints qualitative signatures of topological superconductivity on the junction's interference pattern and the corresponding critical current, even when parity switching processes are abundant. If parity relaxes to minimize the energy, the critical current remains finite at any magnetic flux contrary to conventional symmetric junctions. Still more striking signatures appear if parity instead flips randomly on suitably long time scales—multiple critical currents are visible in the current-voltage traces, and the lower critical current vanishes at zero flux provided the fractional

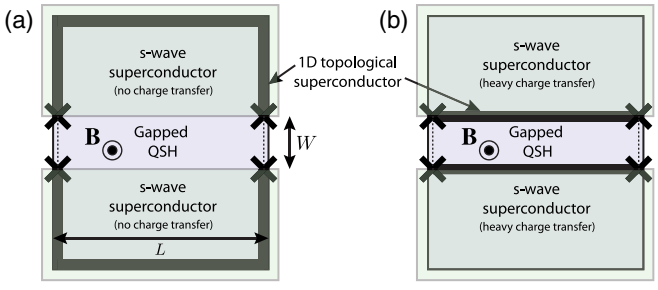

FIG. 1 (color online). Extended QSH Josephson junctions that host 1D topological superconductivity. Topological superconductors reside either (a) at the outer boundary or (b) across the barrier depending on whether the superconductors dope the contacted QSH regions.

Josephson currents dominate. These results highlight relatively simple dc measurements that can reveal 1D topological superconductivity in QSH junctions and related platforms.

Extended Josephson junction model.—Following Ref. [18] we consider two s-wave superconductors deposited on a QSH material to create an extended Josephson junction of barrier width W and length L (see Fig. 1). Suppose first that the QSH system's chemical potential resides everywhere in the bulk gap, and that the superconductors merely induce pairing via the proximity effect. The edge states along the perimeter then form 1D topological superconductors [7] that hybridize at the junction as Fig. 1(a) illustrates. Effectively, the bulk behaves as an SIS junction, while the edges form two parallel SNS junctions that mediate the majority of the current. This picture is supported by the interference pattern observed in HgTe junctions similar to those examined here [18]. Because of work-function mismatch, however, we expect that in practice the superconductors additionally transfer charge and shift the local Fermi level in the contacted QSH regions well into the bulk bands (though the barrier can still remain depleted). In this scenario one can always change the sign of the mass for the heavily doped regions without closing a gap. The outer regions then admit a trivial band structure—hence, edge states occur only at the boundary of the smaller QSH insulator comprising the barrier. As shown in Fig. 1(b) these edge modes form 1D topological superconductors due to proximity with the adjacent superconductors; their hybridization yields the same physics as in Fig. 1(a).

For simplicity, we assume negligible edge-state penetration depth and $W \ll \xi$ and $L \gg \xi$ throughout, with ξ the coherence length of the 1D topological superconductors. In this limit the left or right junction ends each support a single Andreev bound state with energy $(-1)^{p_{L/R}}\Delta\cos(\delta\phi_{L/R}/2)$. Here, Δ is the induced pairing energy while $p_{L/R}$ and $\delta\phi_{L/R}$, respectively, denote the parity and phase difference at the left and right sides. Generally, $\delta\phi_{L/R}$ follow from the phase difference ϕ between the two superconductors and the number of flux quanta $f = \Phi/(h/2e)$ threading the barrier—i.e., $\delta\phi_L = \phi$ and $\delta\phi_R = \phi + 2\pi f$. Defining a vector $\mathbf{p} = (p_L, p_R)$, the bound states together contribute an energy

$$E_{\mathbf{p}}(\phi, f) = \Delta[(-1)^{p_L}\cos(\phi/2) + (-1)^{p_R}\cos(\phi/2 + \pi f)] \tag{1}$$

and a Josephson current $I_{\mathbf{p}}(\phi, f) = (e/\hbar)\partial_\phi E_{\mathbf{p}}(\phi, f)$. Note that the bound-state energies merge with the continuum at isolated values of $\delta\phi_{L/R}$; thus, quasiparticles above the gap constitute one important parity-switching source. One can, however, mitigate this particular switching mechanism by energetically isolating the bound states via in-plane magnetic fields [7], or with interactions in wider junctions [37].

We consider a current-biased junction and extract the I-V characteristics using an overdamped RCSJ model [38]. The total injected current I derives from two parallel channels: the Josephson current and resistive sources such as normal quasiparticles characterized by a resistance R. The former—which we temporarily assume consists only of $I_{\mathbf{p}}$—shunts the resistive component $I_N = V/R = \hbar\dot{\phi}/(2eR)$ provided the junction does not generate voltage. Between two parity-switching events the phase ϕ thus evolves according to

$$I = I_{\mathbf{p}}(\phi, f) + \frac{\hbar}{2eR}\dot{\phi} + \zeta(t), \tag{2}$$

where the last term reflects a thermal noise current satisfying $\langle\zeta(t)\zeta(t')\rangle = 2T/R\delta(t - t')$ (T denotes the junction temperature; throughout we assume $T \ll \Delta$). Equation (2) describes a strongly damped particle with coordinate ϕ in a "tilted washboard" potential $U_{\mathbf{p}}(\phi, f) = E_{\mathbf{p}}(\phi, f) - \hbar I\phi/e$. For sufficiently small I the potential favors pinning the particle to one of its minima. Random thermal noise allows the particle to escape over the barrier [39], whereupon the frictional force $\hbar\dot{\phi}/2eR$ causes relaxation to a new minimum on a time scale proportional to $\tau_R \equiv \hbar^2/(4e^2R\Delta)$. No minima exist above a parity-dependent critical current; the particle then rolls unimpeded down the potential, generating a substantial voltage.

Parity-switching events transfer the particle between different tilted washboard potentials ($U_{\mathbf{p}} \to U_{\mathbf{p}'}$) and thus provide an additional route for the phase ϕ to diffuse even at zero temperature. Our goal now is to quantify the effects of parity switching on transport in various interesting regimes.

Fokker-Planck analysis.—To this end let $\mathcal{P}_{\mathbf{p}}(\phi, t)$ be the distribution function that describes the probability of finding the system with parities $\mathbf{p}$ and phase ϕ at time t. This function obeys a generalized Fokker-Planck equation:

$$\partial_t\mathcal{P}_{\mathbf{p}} = \frac{1}{\tau_R\Delta}\partial_\phi[\partial_\phi U_{\mathbf{p}}/2 + T\partial_\phi]\mathcal{P}_{\mathbf{p}} + \sum_{\mathbf{p}'}[W_{\mathbf{p}'\to\mathbf{p}}\mathcal{P}_{\mathbf{p}'} - W_{\mathbf{p}\to\mathbf{p}'}\mathcal{P}_{\mathbf{p}}], \tag{3}$$

where the first line describes thermal phase diffusion along the tilted washboard potential $U_{\mathbf{p}}$ with fixed parity [39,40] while the second incorporates parity switching with rates $W_{\mathbf{p}\to\mathbf{p}'}$. Equation (3) implicitly assumes that parity-flip processes do not involve an instantaneous change in the phase ϕ; this holds provided the time scale for such events is the shortest in the problem. We further postulate a phenomenological parity-switching mechanism whereby a particle bath connected to the junction allows electrons to tunnel between the bound states and the continuum of bulk excitations, localized states, and other particle sources. We model the corresponding transition rate from parity configuration $\mathbf{p}$ to $\mathbf{p}'$ by

$$W_{\mathbf{p}\to\mathbf{p}'}(\phi, f) = \frac{n[(U_{\mathbf{p}'}(\phi, f) - U_{\mathbf{p}}(\phi, f))/T_b]}{\tau} \times [\delta_{p_R,p'_R}\delta_{p_L,1-p'_L} + \delta_{p_R,1-p'_R}\delta_{p_L,p'_L}], \tag{4}$$

with $1/\tau$ the typical parity-switching rate, $n[x] = (e^x + 1)^{-1}$ the Fermi distribution function, and T_b the bath temperature (which can differ from the junction temperature T). We only consider independent parity flips at the two junction sides—hence the Kronecker delta's in Eq. (4).

The transition rate follows from Fermi's golden rule (for details see the Supplemental Material [41]), where $1/\tau$ is the rate in which electrons transfer between the particle sources and the junction, and T_b corresponds to the window of available energies carried by them. The limit $T_b \sim T \ll \Delta$, for instance, describes hopping between the junction and localized states in the bulk [7]. In contrast, quasiparticles in the superconductor that can enter with a large energy range correspond to the limit $T_b \to \infty$. The latter includes the enhanced quasiparticle poisoning occurring when the bound states merge with the continuum.

The junction's dc voltage V is determined by stationary solutions of Eq. (3). More precisely, the Josephson relation along with Eq. (2) yield

$$V = \frac{\hbar}{2e}\langle\dot{\phi}\rangle = \frac{\hbar}{2e}\sum_{\mathbf{p}}\int_0^{4\pi} d\phi\dot{\phi}\mathcal{P}_{\mathbf{p}}(\phi)$$
$$= R\sum_{\mathbf{p}}\int_0^{4\pi} d\phi[I - I_{\mathbf{p}}(\phi, f)]\mathcal{P}_{\mathbf{p}}(\phi). \quad (5)$$

Determining the I-V characteristics thus reduces to solving Eq. (3) for the steady-state distribution function $\mathcal{P}_{\mathbf{p}}(\phi)$, which is readily achieved numerically by descretizing ϕ. Below we briefly discuss the solution with conserved parity ($1/\tau = 0$) and then address the more realistic case where parity switching occurs.

When the parities $\mathbf{p}$ are conserved the generalized Fokker-Planck equation admits four steady-state solutions—one for each parity sector. The solutions coincide with the known Ambegaokar-Halperin expressions [39] evaluated with an unconventional current-phase relation $I_{\mathbf{p}}(\phi, f)$. At $T = 0$ the voltage follows as [38,39]

$$V = \Theta(I - I_{\mathbf{p},c})R\sqrt{I^2 - I_{\mathbf{p},c}^2}, \quad (6)$$

where $\Theta(x)$ is the Heaviside step function and the critical currents are $I_{\mathbf{p},c} = e\Delta|\cos(\pi f/2)|/\hbar$ for $p_R = p_L$ and $I_{\mathbf{p},c} = e\Delta|\sin(\pi f/2)|/\hbar$ for $p_R \neq p_L$. Thermally induced 4π phase slips at fixed $\mathbf{p}$ produce a finite voltage at $T > 0$ even for $I < I_{\mathbf{p},c}$. Figures 2(a) and 2(b), respectively, illustrate the low-temperature interference patterns in the even- and odd-parity sectors (the color scale represents the voltage V). Both cases exhibit an anomalous two-flux-quanta periodicity—a striking yet fragile fingerprint of topological superconductivity. Indeed this property is spoiled by any finite switching rate $1/\tau \neq 0$, which in our setup will *always* arise due to mixing with continuum quasiparticles and other noise sources. Fortunately, as we now describe other signatures of topological superconductivity nevertheless persist.

For $1/\tau \neq 0$ Eq. (3) admits only one stationary solution due to parity flip processes. Consider first $T_b \ll \Delta$ where the transition rates in Eq. (4) depend strongly on the relative energies in different parity sectors. The behavior then resembles that of a thermalized junction: to a good approximation parities switch only at energy crossings and adjust so that the system follows a washboard potential $U(\phi, f) = \min_{\mathbf{p}} U_{\mathbf{p}}(\phi, f)$ corresponding to a minimum

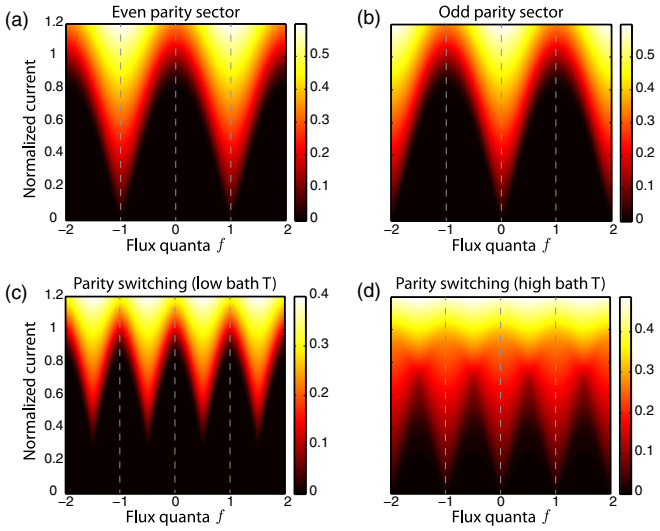

FIG. 2 (color online). Interference patterns in (a),(b) the parity-conserving limit and (c),(d) with parity switching at low ($T_b = 0.02\Delta$) and high ($T_b = 100\Delta$) bath temperature. The color scale indicates voltage in units of $2eR\Delta/\hbar$ while current is normalized by $e\Delta/\hbar$. Data correspond to (a),(b) $T = 0.05\Delta$, (c) $T = 0.02\Delta$, $\tau = 50\tau_R$, and (d) $T = 0.02\Delta$, $\tau = 5\tau_R$.

energy. The $T \to 0$ and $T_b \to 0$ critical current—i.e., the maximal I for which $\partial_\phi U_{\mathbf{p}}(\phi, f) = 0$ admits a solution—follows as $I_c = e\Delta/\hbar \max\{\cos^2(\pi f/2), \sin^2(\pi f/2)\}$. Figure 2(c) displays the numerically computed interference pattern at small but finite T and T_b (which includes thermal phase slips that smear the critical current, as in conventional junctions). The critical current clearly remains finite for all fluxes and, roughly, follows the larger of the critical currents present in the parity-conserving cases shown in Figs. 2(a) and 2(b). Here the absence of nodes is a remnant of the unconventional current-phase relation rooted in topological superconductivity. Other node-lifting sources also, of course, exist but can be distinguished from this mechanism as discussed below.

Finally, we analyze the most interesting limit—$T_b \gg \Delta$, where the parities fluctuate randomly, independent of the initial and final energies, on a time scale τ. Here there are three distinct current regimes separated by the critical currents $I_{c1} = \min_{\mathbf{p}} I_{\mathbf{p},c}$ and $I_{c2} = \max_{\mathbf{p}} I_{\mathbf{p},c}$. For $I < I_{c1}$ local minima exist in the washboard potentials $U_{\mathbf{p}}$ for all four parity sectors. Nevertheless, even at $T = 0$—where thermal diffusion is absent—the phase ϕ can still transform between minima of $U_{\mathbf{p}}$ via parity-switching events; see Figs. 3(a) and 3(b). The voltage resulting from such processes depends on the ratio of τ to the typical time τ_{rel} required for ϕ to relax to a washboard-potential minimum following a parity flip:

$$\tau_{\mathrm{rel}} \sim \max_{\mathbf{p}} \frac{\hbar}{eR\sqrt{I_{\mathbf{p},c}^2 - I^2}}. \quad (7)$$

(A similar time scale emerges in the ac fractional Josephson effect [36].)

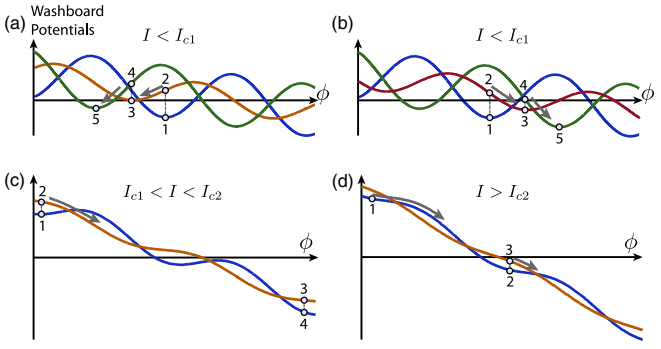

FIG. 3 (color online). Washboard potentials for select parity sectors in the three high-bath-temperature current regimes. For low currents $I < I_{c1}$ consecutive parity flips can mediate $\pm 2\pi$ phase slips as in (a) and (b). In (c) and (d) a steady phase drift always occurs.

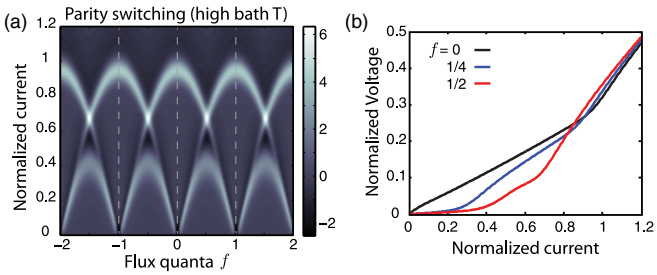

FIG. 4 (color online). (a) Color plot of d^2V/dI^2 and (b) voltage-current line cuts corresponding to the high-bath-temperature data in Fig. 2(d). The two critical currents I_{c1} and I_{c2} are clearly visible in both plots. Voltage and current are respectively expressed in units of $2eR\Delta/\hbar$ and $e\Delta/\hbar$.

For $\tau \gg \tau_{\rm rel}$ the phase ϕ has sufficient time to reach the nearest minimum of the new potential before parity switches again. After two consecutive parity flips ϕ either returns to its initial value or, as Figs. 3(a) and 3(b) illustrate, shifts by $\pm 2\pi$. The 2π and -2π phase changes occur with essentially equal probability when $T_b \gg \Delta$, and, moreover, contribute equal but opposite voltages. Hence these processes cancel one another in the dc limit. In other words, parity switching events generate telegraph noise in the voltage with equal probability of positive and negative signals that time average to zero. As the current approaches I_{c1}, the relaxation time $\tau_{\rm rel}$ grows and eventually exceeds the parity-flip time τ. Consecutive switching events then occur before the phase relaxes to the potential minima; the result is a net diffusion of ϕ down the washboard potentials, producing a finite voltage. This argument implies that in the limit $\tau \lesssim \hbar/(eRI_{c1}) \sim \tau_R$ any current generates a nonzero voltage—i.e., the critical current vanishes.

With currents between I_{c1} and I_{c2} only two of the washboard potentials exhibit stable minima. Because of the high bath temperature, the phase ϕ can escape from one of these minima via a parity-switching event into a potential without any minima, producing a steady drift of ϕ. The drift ceases only when a subsequent parity flip retraps the phase; see Fig. 3(c) for an illustration. Assuming $\tau \gg \tau_{\rm rel}$, the phase drift generates a finite dc voltage $V \approx \mathcal{F}_{\rm drift} R\sqrt{I^2 - I_{c1}^2}$ with $\mathcal{F}_{\rm drift}$ the fraction of time spent in potentials without minima ($\mathcal{F}_{\rm drift} \approx 1/2$ when $T_b \gg \Delta$). For currents close to I_{c2} the phase relaxation time $\tau_{\rm rel}$ exceeds τ; the phase can then essentially never reach a minimum due to frequent parity flips. An additional voltage contribution thus appears, which smears the voltage as a function of current near I_{c2}—just as in the region near I_{c1} discussed earlier.

Above I_{c2} none of the bands support minima, and the phase ϕ drifts continuously as in Fig. 3(d). The instantaneous drift velocity and hence also the voltage are nonetheless parity dependent. It follows that parity switching events, on average, produce a voltage $V \approx \mathcal{F}'_{\rm drift} R\sqrt{I^2 - I_{c1}^2} + (1 - \mathcal{F}'_{\rm drift}) R\sqrt{I^2 - I_{c2}^2}$. Here $\mathcal{F}'_{\rm drift}$ and $1 - \mathcal{F}'_{\rm drift}$ denote the fraction of time the phase spends in the potentials with critical currents I_{c1} and I_{c2}, respectively.

We thus arrive at the following overall picture for the high-bath-temperature case. When $\tau \gg \tau_R$ the dc voltage remains negligible as long as $I < I_{c1} = \min_{\mathbf{p}} I_{\mathbf{p},c}$. That is, contrary to the limit $T_b \ll \Delta$ the (lower) critical current as a function of flux follows the minimum of the critical currents associated with the four parity sectors. Furthermore, the critical current vanishes at zero flux and is maximal at one-half flux quantum—precisely as in a π junction [see Fig. 2(d)]. For $I > I_{c1}$ the voltage is far from featureless—a second critical current $I_{c2} = \max_{\mathbf{p}} I_{\mathbf{p},c}$ also appears, reflecting the multiple parity sectors. This feature becomes prominent upon examining d^2V/dI^2 [Fig. 4(a)] as well as specific voltage-current line cuts [Fig. 4(b)]. Thus, long parity-flip times τ allow one to image the critical currents in all parity sectors. Rapid parity flipping with $\tau \lesssim \tau_R$, however, renders the junction resistive at any flux and yields identically zero critical current.

Discussion.—Our study of extended QSH Josephson junctions reveals that parity switching processes, although destructive to the critical current's anomalous periodicity, generate new fingerprints of the underlying topological superconductors expected to form. Surprisingly, stronger poisoning actually enhances the signatures in the critical current (as long as parity fluctuates on sufficiently long time scales). We expect the results to apply quite generally—even when the actual switching mechanism differs from our model. For instance, if the bound-state energies approach the continuum states near Δ then bulk quasiparticles can easily mediate parity flips [36]. We verified numerically that qualitatively similar behavior to the high-T_b limit arises when switching occurs predominantly at energies near Δ.

While our analysis has so far included only 4π-periodic current contributions, it is important to note that conventional 2π-periodic components $\propto \sin \delta\phi_{R/L}$ generically flow in parallel (though their magnitudes may be small). The Supplemental Material [41] addresses the consequences of such terms. With low bath temperatures their effects are decidedly minor—the lifted nodes in Fig. 2(c) survive even for quite large conventional currents. More significant effects occur at high bath temperature. There, the new terms lead

to deviations from the π-junction behavior mimicked in Fig. 2(d). The resulting interference pattern nevertheless still remains anomalous. Most importantly multiple critical currents remain visible in the current-voltage relation. The critical current, as with low bath temperatures, also remains finite for any magnetic field.

The absence of nodes in the critical current at half-integer flux quanta thus survives quite generally from the interplay between fractional Josephson physics and parity switching (we include a tentative comparison with experiment regarding this feature in the Supplemental Material [41]; see also Ref. [42] for a somewhat related mechanism). To provide a compelling indicator of topological superconductivity, however, the ability to experimentally distinguish from other node-lifting mechanisms such as current asymmetry is essential. This may be achieved by introducing a strong *in-plane* magnetic field, which can force the 1D topological superconductors at the junction into a trivial phase [7]. Therefore, observing the controlled destruction and revival of nodes as one varied the in-plane field strength would likely rule out alternative mechanisms and provide strong evidence for topological superconductivity.

We are indebted to D. Clarke, J. Meyer, J. Sau, A. Stern, D. van Harlingen, and especially B. Halperin, S. Hart, and H. Ren for enlightening discussions. We also acknowledge funding from the NSF through Grants No. DMR-1341822 (S.-P. L. and J. A.) and No. DMR-1206016 (A. Y.), the Alfred P. Sloan Foundation (J. A.), a grant from Microsoft Corporation (A. Y.), and the Caltech Institute for Quantum Information and Matter, an NSF Physics Frontiers Center, with support of the Gordon and Betty Moore Foundation. A. Y. is also supported by the STC Center for Integrated Quantum Materials, NSF Grant No. DMR-1231319.

[1] A. Y. Kitaev, Sov. Phys. Usp. **44**, 131 (2001).
[2] C. W. J. Beenakker, Annu. Rev. Condens. Matter Phys. **4**, 113 (2013).
[3] J. Alicea, Rep. Prog. Phys. **75**, 076501 (2012).
[4] M. Leijnse and K. Flensberg, Semicond. Sci. Technol. **27**, 124003 (2012).
[5] T. D. Stanescu and S. Tewari, J. Phys. Condens. Matter **25**, 233201 (2013).
[6] C. Nayak, S. H. Simon, A. Stern, M. Freedman, and S. Das Sarma, Rev. Mod. Phys. **80**, 1083 (2008).
[7] L. Fu and C. L. Kane, Phys. Rev. B **79**, 161408(R) (2009).
[8] R. M. Lutchyn, J. D. Sau, and S. Das Sarma, Phys. Rev. Lett. **105**, 077001 (2010).
[9] Y. Oreg, G. Refael, and F. von Oppen, Phys. Rev. Lett. **105**, 177002 (2010).
[10] A. Cook and M. Franz, Phys. Rev. B **84**, 201105 (2011).
[11] T.-P. Choy, J. M. Edge, A. R. Akhmerov, and C. W. J. Beenakker, Phys. Rev. B **84**, 195442 (2011).
[12] S. Nadj-Perge, I. K. Drozdov, B. A. Bernevig, and A. Yazdani, Phys. Rev. B **88**, 020407 (2013).
[13] A. C. Potter and P. A. Lee, Phys. Rev. B **83**, 184520 (2011).
[14] B. A. Bernevig, T. L. Hughes, and S.-C. Zhang, Science **314**, 1757 (2006).
[15] M. Konig, S. Wiedmann, C. Brune, A. Roth, H. Buhmann, L. W. Molenkamp, X.-L. Qi, and S.-C. Zhang, Science **318**, 766 (2007).
[16] A. Roth, C. Brune, H. Buhmann, L. W. Molenkamp, J. Maciejko, X.-L. Qi, and S.-C. Zhang, Science **325**, 294 (2009).
[17] K. C. Nowack, E. M. Spanton, M. Baenninger, M. König, J. R. Kirtley, B. Kalisky, C. Ames, P. Leubner, C. Brüne, H. Buhmann, L. W. Molenkamp, D. Goldhaber-Gordon, and K. A. Moler, Nat. Mater. **12**, 787 (2013).
[18] S. Hart, H. Ren, T. Wagner, P. Leubner, M. Mühlbauer, C. Brüne, H. Buhmann, L. W. Molenkamp, and A. Yacoby, Nat. Phys. **10**, 638 (2014).
[19] C. Liu, T. L. Hughes, X.-L. Qi, K. Wang, and S.-C. Zhang, Phys. Rev. Lett. **100**, 236601 (2008).
[20] L. Du, I. Knez, G. Sullivan, and R.-R. Du, arXiv:1306.1925.
[21] E. M. Spanton, K. C. Nowack, L. Du, R.-R. Du, and K. A. Moler, Phys. Rev. Lett. **113**, 026804 (2014).
[22] I. Knez, R.-R. Du, and G. Sullivan, Phys. Rev. Lett. **109**, 186603 (2012).
[23] S. Mi, D. I. Pikulin, M. Wimmer, and C. W. J. Beenakker, Phys. Rev. B **87**, 241405 (2013).
[24] C. W. J. Beenakker, J. M. Edge, J. P. Dahlhaus, D. I. Pikulin, S. Mi, and M. Wimmer, Phys. Rev. Lett. **111**, 037001 (2013).
[25] F. Crepin, B. Trauzettel, and F. Dolcini, Phys. Rev. B **89**, 205115 (2014).
[26] A. M. Black-Schaffer and J. Linder, Phys. Rev. B **83**, 220511 (2011).
[27] D. M. Badiane, M. Houzet, and J. S. Meyer, Phys. Rev. Lett. **107**, 177002 (2011).
[28] L. Jiang, D. Pekker, J. Alicea, G. Refael, Y. Oreg, and F. von Oppen, Phys. Rev. Lett. **107**, 236401 (2011).
[29] Q. Meng, V. Shivamoggi, T. L. Hughes, M. J. Gilbert, and S. Vishveshwara, Phys. Rev. B **86**, 165110 (2012).
[30] L. Jiang, D. Pekker, J. Alicea, G. Refael, Y. Oreg, A. Brataas, and F. von Oppen, Phys. Rev. B **87**, 075438 (2013).
[31] M. Houzet, J. S. Meyer, D. M. Badiane, and L. I. Glazman, Phys. Rev. Lett. **111**, 046401 (2013).
[32] C. W. J. Beenakker, D. I. Pikulin, T. Hyart, H. Schomerus, and J. P. Dahlhaus, Phys. Rev. Lett. **110**, 017003 (2013).
[33] S. Barbarino, R. Fazio, M. Sassetti, and F. Taddei, New J. Phys. **15**, 085025 (2013).
[34] S.-F. Zhang, W. Zhu, and Q.-F. Sun, J. Phys. Condens. Matter **25**, 295301 (2013).
[35] F. Crepin and B. Trauzettel, Phys. Rev. Lett. **112**, 077002 (2014).
[36] D. M. Badiane, L. I. Glazman, M. Houzet, and J. S. Meyer, C.R. Phys. **14**, 840 (2013).
[37] F. Zhang and C. L. Kane, Phys. Rev. Lett. **113**, 036401 (2014).
[38] M. Tinkham, *Introduction to Superconductivity*, 2nd ed. (Dover, Mineola, New York, 1996).
[39] V. Ambegaokar and B. I. Halperin, Phys. Rev. Lett. **22**, 1364 (1969).
[40] H. Risken, *The Fokker-Planck Equation* (Springer-Verlag, Berlin, Heidelberg, 1989).
[41] See Supplemental Material at http://link.aps.org/supplemental/10.1103/PhysRevLett.113.197001 for a derivation of the Fokker-Planck equation with parity switching, an analysis of additional supercurrent sources, and a comparison with existing experiments.
[42] A. C. Potter and L. Fu, Phys. Rev. B **88**, 121109 (2013).